Echocardiographic Ischemic Memory Imaging Through Complement-Mediated Vascular Adhesion of Phosphatidylserine-Containing Microbubbles

Brian Mott, MD,[a] William Packwood, BS,[a] Aris Xie, MS,[a] J. Todd Belcik, BS, RCS, RDCS,[a] Ronald P. Taylor, PHD,[b] Yan Zhao, MD,[a] Brian P. Davidson, MD,[a] Jonathan R. Lindner, MD[a]

ABSTRACT

OBJECTIVES This study hypothesized that microvascular retention of phosphatidylserine-containing microbubbles (MB-PS) would allow detection of recent but resolved myocardial ischemia with myocardial contrast echocardiographic (MCE) molecular imaging.

BACKGROUND Techniques for ischemic memory imaging which can detect and spatially assess resolved myocardial ischemia are being developed for rapid evaluation of patients with chest pain.

METHODS MCE molecular imaging with MB-PS was performed 1.5 h, 3.0 h, and 6.0 h after brief (10 min) myocardial ischemia in mice; data were compared to selectin-targeted microbubbles. MCE molecular imaging with Sonazoid (GE Healthcare, Amersham, United Kingdom), a commercially produced phosphatidylserine (PS) – containing agent, was performed in separate mice at 1.5 h and 3.0 h after ischemia-reperfusion; and in dogs undergoing 135 min of ischemia and 60 min of reflow as well as in closed-chest nonischemic control dogs. The mechanism for MB-PS attachment was assessed by intravital microscopy of post-ischemic muscle and by flow cytometry analysis of cell-MB interactions.

RESULTS In mice undergoing ischemia-reperfusion without infarction, signal enhancement in the risk area for MB-PS and p-selectin glycoprotein ligand-1–targeted microbubbles was similar at reflow times of 1.5 h (23.3 ± 7.3 IU vs. 30.7 ± 4.1 IU), 3.0 h (42.2 ± 6.2 IU vs. 33.9 ± 7.4 IU), and 6.0 h (24.1 ± 4.3 IU vs. 25.5 ± 4.7 IU). For both agents, signal in the risk area was significantly ($p < 0.05$) higher than remote region at all reflow times. Sonazoid also produced strong risk area enhancement at 1.5 h (34.7 ± 5.0 IU) and 3.0 h (52.5 ± 4.5 IU) which was approximately 3-fold greater than in the control region, and which correlated spatially with the microsphere-derived risk area. In dogs, Sonazoid signal in the risk area was >5-fold higher than in closed-chest control myocardium (42.2 ± 8.1 IU vs. 7.9 ± 3.3 IU; $p < 0.001$). Mechanistic studies indicated that MB-PS attached directly to venular endothelium and adherent leukocytes which was dependent on serum complement components C1q and C3.

CONCLUSIONS Ischemic memory imaging with MCE is possible using MB-PS which may obviate the need for ligand-directed targeting. (J Am Coll Cardiol Img 2016;9:937–46) © 2016 by the American College of Cardiology Foundation.

The diagnosis of acute coronary syndrome (ACS) in symptomatic patients relies on clinical history, laboratory evaluation, and electrocardiogram which, except in the case of ST-segment elevation myocardial infarction, are often nondiagnostic on initial evaluation (1,2). To address this limitation, molecular imaging techniques for detecting ischemia-related molecular profiles

have been developed and may be useful for diagnosing ACS when initial tests are negative or when ischemia has resolved and not resulted in much myocardial necrosis (3). They could potentially also identify high-risk individuals based on the spatial extent of the area at risk.

Ultrasound is a practical approach for ischemic memory imaging because it is portable and rapid. Molecular imaging of resolved ischemia without infarction has been performed with myocardial contrast echocardiography (MCE) in rodent and nonhuman primate models using microbubbles targeted to the selectin family of endothelial cell adhesion molecules that are rapidly expressed in response to ischemia (4-7). Clinical translation of this approach has been slowed by the arduous regulatory process of testing efficacy and safety of a human-ready microbubble agent bearing a biologically active ligand. In this study, we propose an alternative approach through modulation of microbubble lipid shell content. Complement-mediated adhesion of lipid-shelled microbubbles to activated leukocytes and endothelial cells occurs in areas of inflammation (8-10). This process is amplified by the presence of anionic lipids, especially phosphatidylserine (PS) in the shell (11). Phosphatidylserine microbubbles (MB-PS) have been used to noninvasively image inflammation in both chronic limb ischemia and severe acute myocardial infarction (12,13).

In this study we hypothesized that MB-PS can identify and assess the spatial extent of recent but resolved myocardial ischemia without infarction. Additional aims of the study were to: 1) compare MB-PS to a selectin-targeted microbubble agent bearing recombinant human p-selectin glycoprotein ligand-1 (PSGL-1); 2) evaluate the potential for performing ischemic memory imaging with a commercially produced PS-containing microbubble already used in humans; and 3) to further characterize the mechanism for MB-PS adhesion in regions of ischemia.

METHODS

MICROBUBBLE PREPARATION.
Lipid-shelled MB-PS were prepared by sonication of a decafluorobutane gas-saturated aqueous suspension of 2 mg/ml distearoylphosphatidylcholine, 1 mg/ml polyoxyethylene-40-stearate, and 0.3 mg/ml distearoyl phosphatidylserine (Avanti Polar Lipids, Alabaster,

Alabama). For p-selectin glycoprotein ligand-1–targeted microbubbles (MB-PSGL-1), biotinylated microbubbles were prepared and a PSGL-1 dimeric fusion protein on a human immunoglobulin G1 (Y's Therapeutics, Tokyo, Japan) was conjugated to the surface using a streptavidin link as previously described (6). For intravital microscopy and flow cytometry, MB-PS was fluorescently labeled by the addition of dioctadecyl tetramethylindocarbocyanine (DiI) or dioctadecyloxacarbocyanine (DiO) perchlorate. Clinical grade commercially produced decafluorobutane microbubbles with a shell composed of egg PS (Sonazoid, GE Healthcare, Amersham, United Kingdom) were reconstituted according to manufacturer's instructions. Microbubble size distribution and concentration was measured by electrozone sensing (Multisizer III, Beckman Coulter, Brea, California). Zeta potential was determined by measurement of their electrophoretic mobility (ZetaPALS, Brookhaven Instruments, Holtsville, New York) at pH 7.4.

MURINE MODEL OF MYOCARDIAL ISCHEMIA.
Studies were approved by the Animal Care and Use Committee at Oregon Health & Science University. Brief myocardial ischemia or sham procedure was performed in C57Bl/6 mice (Jackson Labs, Bar Harbor, Maine) 10 to 15 weeks of age. Mice were anesthetized with inhaled isoflurane and placed on positive-pressure ventilation. A left lateral thoracotomy was performed and a 8-0 Prolene suture was placed around the left anterior descending (LAD) coronary artery. For the ischemic group, the ligature was secured for 10 min to produce myocardial ischemia confirmed by ST-segment elevation on electrocardiogram. The ligature was released and left in place, the chest wall was closed, and mice were extubated. For sham-treated animals, the ligature was placed but not secured. To exclude the presence of infarction, at the end of each study high-frequency (30 MHz) echocardiography (Vevo 770, Visualsonics, Toronto, Canada) was performed to exclude wall motion abnormality and the heart slice corresponding to the short-axis imaging plane was stained with 2,3,5-triphenyltetrazolium chloride.

MOLECULAR IMAGING.
MCE molecular imaging of the midventricular short-axis plane was performed with a linear-array probe (Sequoia, Siemens Medical Systems, Mountainview, California) using multipulse phase-inversion and amplitude-modulation imaging at 7 MHz, a mechanical index of 1.4, and a dynamic range of 55 dB. End-systolic images were acquired 8 min after intravenous injection of microbubbles (5×10^6). Signal from retained microbubbles alone was determined as previously described by digital

subtraction of the signal from the residual freely circulating microbubbles in the blood pool (6,9). Fundamental 2-dimensional imaging at 14 MHz after each MCE molecular imaging sequence was used to help define epicardial and endocardial borders. Intensity from retained microbubbles was measured from regions-of-interest placed over remote non-ischemic nonattenuated myocardium and over the risk area determined by microsphere technique.

EXPERIMENTAL GROUPS FOR ISCHEMIC MEMORY IMAGING IN MICE. Protocol 1. MCE molecular imaging with MB-PS and MB-PSGL-1 in random order was performed in mice undergoing myocardial ischemia at 1.5 h and 3.0 h (n = 9), or 6.0 h (n = 11) after reperfusion. For any animals that did not survive to microsphere injection, the risk area was defined by the area of MB-PSGL-1 enhancement because this area correlates closely to that derived from microspheres (5,6).

Protocol 2. In separate mice, MCE molecular imaging with Sonazoid was performed at 1.5 h and 3.0 h after ischemia-reperfusion imaging (n = 11). In 5 of these animals, MCE molecular imaging was also performed with control microbubbles (MB) not containing PS. In all of these experiments, the region of enhancement on MCE molecular imaging was compared spatially to the risk area derived by microsphere technique.

MICROSPHERE-DERIVED RISK AREA. After completion of imaging, animals were placed back on positive-pressure ventilation and the chest was reopened. The LAD ligature was resecured and 1% w/v fluorescently labeled polystyrene microspheres 3 μm to 8 μm in diameter (Duke Scientific Corp., Palo Alto, California) were injected through a 23-g needle placed in the left ventricular apex. A 1-mm thickness short-axis section corresponding to the echocardiographic imaging plane was imaged by fluorescent microscopy. The fluorescent-free risk area and the area of MCE molecular imaging enhancement were separately assessed spatially by readers blinded to animal identity.

CANINE MODEL OF ISCHEMIC MEMORY IMAGING. Molecular imaging with Sonazoid was performed in a canine model of ischemia-reperfusion. Because these experiments were performed as a supplement to another protocol, occlusion duration was sufficiently long to produce a small myocardial infarction and the chest remained open for the entire study duration. In 7 male mongrel dogs (28 kg to 32 kg), the heart was exposed through a left-lateral thoracotomy. Time-of-flight flow probes were placed around the LAD or the left circumflex coronary artery, and 1 of

the 2 arteries was ligated for 135 min. During occlusion, MCE perfusion imaging was performed using a continuous infusion of nontargeted lipid-shelled decafluorobutane microbubbles (1×10^7 min^{-1}) in a midventricular short-axis plane that included a region of akinesis using intermittent high–mechanical index (1.3) imaging with a phased-array transducer (1.3 MHz) and ultraharmonic filtering (Sonos 5500, Philips Ultrasound, Andover, Massachusetts). At 60 min after reflow, 1.5×10^8 Sonazoid microbubbles were injected intravenously and MCE was performed 10 min later using analysis similar to the murine protocols. At 90 min after reflow, MCE perfusion imaging was performed to evaluate microvascular reflow. The perfusion territory of the infarct related artery was measured by MCE during direct injection of contrast in the infarct-related artery. The short-axis slice corresponding to the imaging plane was stained with 2,3,5-triphenyltetrazolium chloride (TTC). The MCE imaging protocol with Sonazoid was performed in an additional 2 control closed-chest dogs not undergoing ischemia and analysis was performed for both the LAD and left circumflex (LCx) region using 2 separate short-axis planes.

INTRAVITAL MICROSCOPY. Intravital microscopy was performed in 4 C57Bl/6 mice as previously described to characterize MB-PS retention in post-ischemic tissue. Ischemia was produced for 15 min by direct pressure applied to the cremasteric feeding pedicle which arrested microvascular erythrocyte transit. At 30 min and 60 min after reperfusion, DiI-labeled MB-PS (1×10^7) were injected intravenously and microbubble retention (n = 60 events) was characterized according to the type of microvessel and cell type of attachment.

FLOW CYTOMETRY. The mechanism of MB-PS interaction with inflammatory cells was assessed by flow cytometry. Heparinized whole blood was obtained from healthy human volunteers. The neutrophil and monocyte leukocyte fractions were separated by density gradient centrifugation and were labeled with allophycocyanin (APC) anti-human CD45 monoclonal antibody (BD Biosciences, San Jose, California). DiO-labeled MB-PS were combined with leukocytes in a 2:1 ratio for 15 min in a total volume of 300 μl using the following incubational milieus: 1) human serum; 2) heat-inactivated serum (56° C for 30 min) to deactivate complement; and 3) either C1q-deficient or C3-deficient human serum (Complement Technology, Inc., Tyler, Texas). Non–serum-dependent interactions were investigated by incubation in phosphate-buffered saline using unaltered leukocytes or leukocytes pre-incubated with human anti-human

CD36 monoclonal antibody (185-1G2, Abcam, Cambridge, United Kingdom), or phosphatidylserine-containing micelles. Flow cytometry (LSRFortessa, Becton Dickinson, San Jose, California) with leukocytes or MB-PS alone were used to determine control fluorescent conditions, to establish exclusion gates (Online Figure 1).

STATISTICAL ANALYSIS. Data were analyzed using Prism (version 5.0, GraphPad Software, San Diego, California). Group-wise differences were assessed by the Mann-Whitney U test for data that were determined to be non-normally distributed by the D'Agostino and Pearson omnibus test. For data with normal distribution, group-wise differences were assessed by one-way analysis of variance with post-hoc Student t test and Bonferroni's correction. For comparisons of microsphere risk area and spatial extent of ischemic memory signal enhancement, bias was assessed using Bland-Altman analysis. Differences were considered significant at $p < 0.05$ (2-sided).

RESULTS

MICROBUBBLE CHARACTERISTICS. The physical and chemical characteristics of each microbubble agent are provided in Table 1. Average diameter did not differ substantially between agents. The zeta potential for MB-PS and Sonazoid were reduced compared to the non-PS-containing agents and was more negative for Sonazoid which contained 100% PS as an excipient.

ISCHEMIC MEMORY IMAGING WITH MB-PS. Ischemia during LAD ligation in all mice was confirmed by ST-segment elevation. Wall thickening in the risk area was reduced compared to a control region at 15 min after reflow ($24 \pm 19\%$ vs. $42 \pm 14\%$; $p = 0.01$), but recovered at 3 h ($37 \pm 10\%$ vs. $42 \pm 14\%$; $p = 0.36$). The spatial extent of the risk area in the ischemia-reperfusion group was $35 \pm 4\%$ of the short-axis area (range 29% to 39%). Irrespective of the duration of reflow, on MCE molecular imaging there was a similar degree of selective enhancement in the risk area for MB-PS and MB-PSGL-1 which was higher than that in the remote control region at each

post-reperfusion interval (Figure 1). Signal enhancement in the control region, which has been attributed to trauma from surgical exposure or remote territory microvascular activation (4,6), tended to be slightly higher for MB-PSGL-1 at 1.5 h and slightly higher for MB-PS at 3.0 h, although differences did not reach statistical significance. There was no evidence for infarction on TTC staining except for a very small epicardial region at the intramyocardial site of suture placement which was deemed to be at a more basal location than the imaging plane.

ISCHEMIC MEMORY IMAGING WITH SONAZOID. In mice undergoing MCE molecular imaging with Sonazoid, the mean risk area by microspheres was $38 \pm 8\%$ (range 22% to 48%). On MCE molecular imaging, there was selective signal enhancement seen in the risk area which was significantly greater than in the control remote region at 1.5 h and 3.0 h after reflow (Figure 2). Similar to the case with MB-PS, signal in the risk area and remote territory were slightly higher at 3.0 h than 1.5 h. Signal from control MBs not containing PS was less than one-half of that seen for Sonazoid at both time intervals. The region of Sonazoid enhancement correlated with that defined by fluorescent microspheres, although there was a slight underestimation by MCE at 1.5 h which was of borderline significance. There was no significant infarction seen on TTC staining in the imaging plane.

In canine experiments, the risk area measured by direct injection of contrast into the infarct-related artery was $35 \pm 9\%$ of short-axis area (range 21% to 49%). Because of prolonged coronary occlusion, a small region of infarction ($9 \pm 7\%$ of short axis area) was detected by TTC staining. Signal enhancement on MCE molecular imaging with Sonazoid was significantly greater in the risk area than remote territory (Figure 3), and tended to be greatest in central portion of the risk area. However, signal enhancement in the remote territory was also relatively high, whereas enhancement was low in closed-chest dogs not undergoing ischemia.

MECHANISM OF MICROBUBBLE RETENTION. Intravital microscopy performed 30 min and 60 min after brief cremasteric ischemia revealed that vascular retention of MB-PS was attributable mostly to direct attachment to the venular endothelium (20% of events) or to adherent inflammatory cells in venules (73% of events) (Online Videos 1 and 2). Attachment to arteriolar endothelium was present but uncommon (7% of events). Flow cytometry revealed that the presence of serum was a critical component for MB-PS attachment to monocytes and neutrophils (Figure 4). Attachment was greatly

TABLE 1 Microbubble Physical and Chemical Properties

	MB	MB-PS	Sonazoid	MB-PSGL-1
Diameter, μm	2.1 ± 0.2	2.1 ± 0.2	2.0 ± 0.1	2.3 ± 0.2
Zeta potential, mV	-3	-29	-80*	-13
PS content, molar %	0	11	100	0

*Data derived from experiments performed previously (22).

MB = control microbubbles; MB-PS = phosphatidylserine microbubbles; MB-PSGL-1 = p-selectin glycoprotein ligand-1– targeted microbubbles; PS = phosphatidylserine.

FIGURE 1 Myocardial Contrast Echocardiographic Ischemic Memory Imaging With Phosphatidylserine Microbubbles and p-Selectin Glycoprotein Ligand-1–Targeted Microbubbles
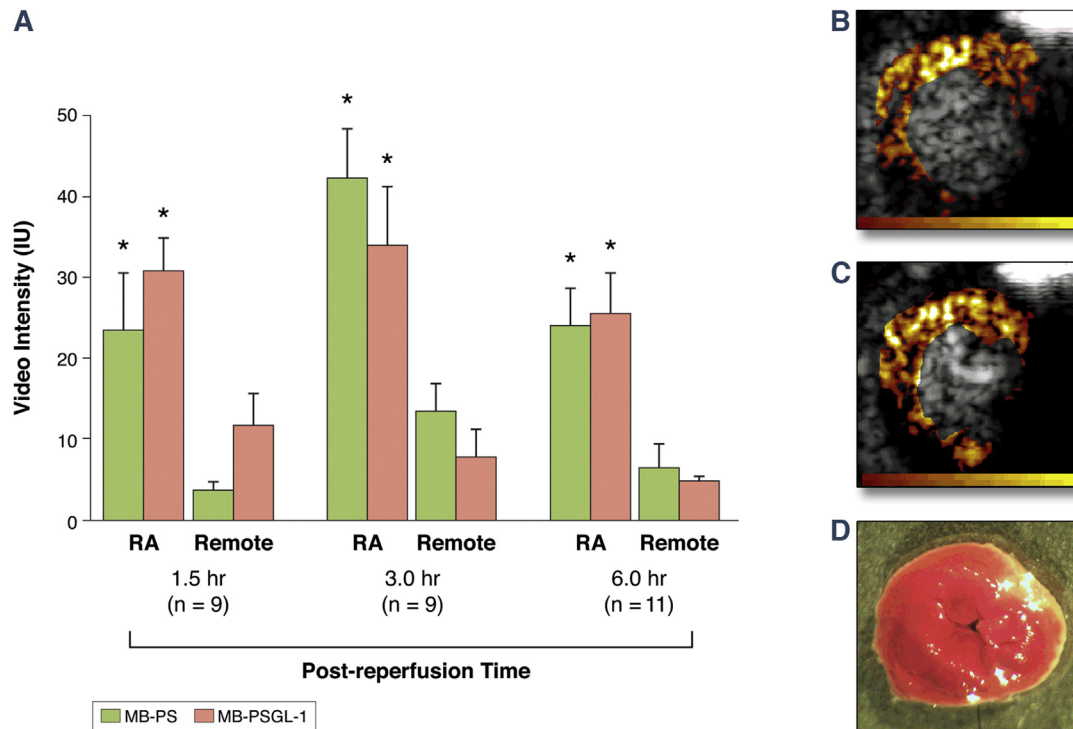
(A) Mean (±SEM) intensity in the risk area (RA) and remote territory at incremental time after reperfusion. (*$p < 0.05$ versus remote.) Examples from a single animal are shown for MCE molecular imaging at 1.5 h for **(B)** phosphatidylserine microbubbles (MB-PS) and **(C)** p-selectin glycoprotein ligand-1–targeted microbubbles (MB-PSGL-1) (color scales at bottom). **(D)** The corresponding triphenyltetrazolium chloride (TTC) staining showing absence of infarction.
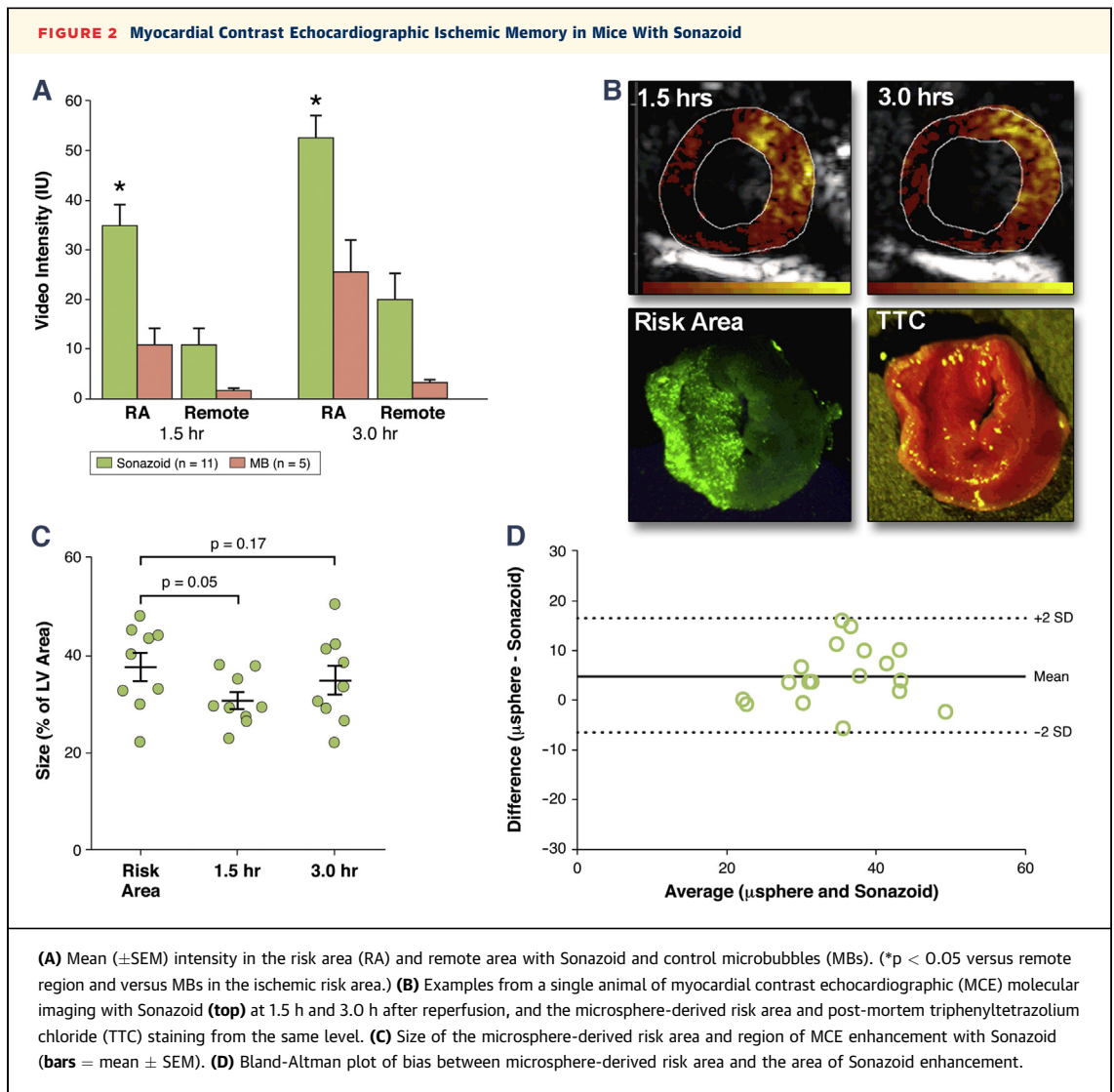
inhibited by using heat-inactivated, C1q-deficient, and C3-deficient serum, indicating the critical role of serum complement. The very small amount of MB-PS attachment to leukocytes in the absence of serum was reduced by pre-incubation with lipid micelles and by CD36 scavenger receptor inhibition.

DISCUSSION

Interest in ischemic memory imaging is predicated on the notion that clinical care can be improved and healthcare costs reduced by techniques that improve the speed and accuracy of risk assessment in patients who present with symptoms suspicious for myocardial ischemia. MCE is an attractive approach for this application because ultrasound is increasingly used in the emergency department for rapid assessment of patients with a variety of conditions, and requires only a short duration to perform. In this study we have demonstrated in pre-clinical models that recent

but resolved myocardial ischemia can be detected and spatially assessed with the relatively simple approach of using lipid microbubbles that do not carry any specific binding ligand but rather that contain PS. The mechanism for post-ischemic enhancement with MB-PS appears to be via the naturally occurring activation of complement which is probably initiated by C1q binding on the negative surface of the microbubbles.

Key determinants for successful implementation of ischemic memory imaging are the ability to detect ischemia without infarction and to detect ischemia long after its resolution. Accordingly, in the murine experiments MCE molecular imaging was performed as long as 6 h after a very brief ischemic insult which did not cause infarction. Unexpectedly, we found that the degree of signal enhancement for MB-PS in the risk area at all post-ischemic time points was similar to obtained using a pan-selectin ligand which has been shown to be useful for ischemic memory

FIGURE 2   Myocardial Contrast Echocardiographic Ischemic Memory in Mice With Sonazoid

(A) Mean (±SEM) intensity in the risk area (RA) and remote area with Sonazoid and control microbubbles (MBs). (*p < 0.05 versus remote region and versus MBs in the ischemic risk area.) **(B)** Examples from a single animal of myocardial contrast echocardiographic (MCE) molecular imaging with Sonazoid **(top)** at 1.5 h and 3.0 h after reperfusion, and the microsphere-derived risk area and post-mortem triphenyltetrazolium chloride (TTC) staining from the same level. **(C)** Size of the microsphere-derived risk area and region of MCE enhancement with Sonazoid (**bars** = mean ± SEM). **(D)** Bland-Altman plot of bias between microsphere-derived risk area and the area of Sonazoid enhancement.

imaging in murine and nonhuman primate models (6,7). Experiments with Sonazoid were performed to confirm that a commercially produced PS-containing microbubble already approved for human use in certain European and Asian countries could produce similar results. In all experiments, there was a reasonable correlation between the spatial extent of the risk area and the area of MCE enhancement even when MCE molecular imaging was performed late after ischemia resolution. This finding is important because the size of the ischemic territory is likely to be an important consideration in the potential clinical application of the technology.

In canine experiments the ischemic duration was longer than in murine studies but resulted in only a very small infarction. We have previously demonstrated that MCE molecular imaging with MB-PS in a canine model of moderate-sized reperfused infarction produces enhancement in the entire risk area early after reflow and that the area of enhancement does depend on time delay from reperfusion to imaging (12). In the current study, we demonstrated that commercially produced Sonazoid provides similar information in a model with minimal infarction.

The clinical potential of MCE molecular imaging for rapid triage in patients is dependent upon high sensitivity (confidence that most ischemic events will be found) and high negative predictive value (confidence that it is safe to discharge patients if tests are negative). Results from this study are reassuring that signal enhancement was seen in all post-ischemic regions. Because the positive predictive value of the test is also important to avoid unnecessary costs and procedures, the signal enhancement seen in the

FIGURE 3 Myocardial Contrast Echocardiographic Ischemic Memory in Dogs With Sonazoid
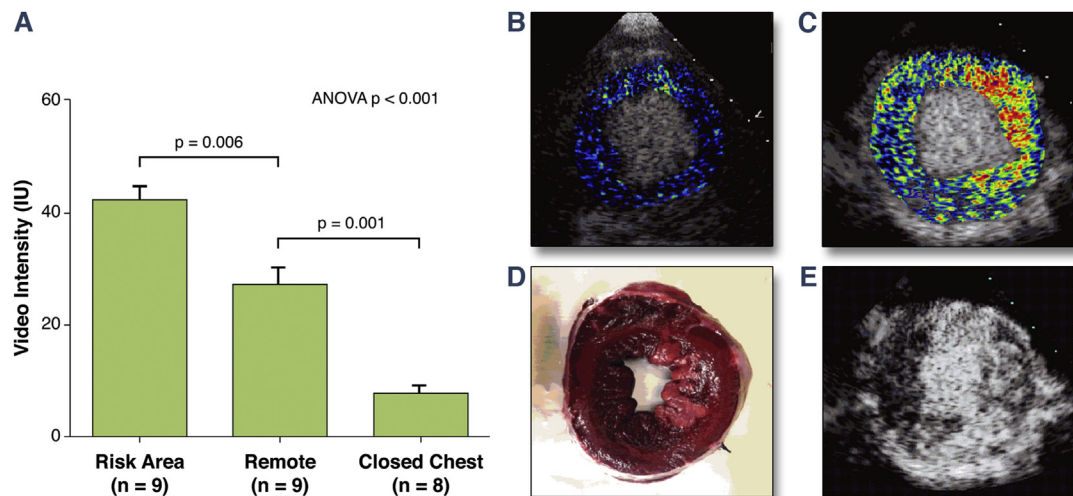
(A) Mean (±SEM) intensity in the risk and remote areas in dogs undergoing ischemia-reperfusion, and in both left anterior descending coronary artery and left circumflex territories together in closed-chest nonischemic controls (n for closed-chest represents region rather than animal number). (B) Example of myocardial contrast echocardiography (MCE) from a closed-chest control animal. (C to E) Examples of MCE, triphenyltetrazolium chloride staining and risk area by method of intracoronary injection of contrast from a single animal undergoing left circumflex ischemia reperfusion. ANOVA = analysis of variance.

control regions in this study is an important consideration. In prior murine studies using selectin-targeted MBs, enhancement in remote territories has been shown to be caused mostly by inflammation from the open-chest models and cardiac manipulation [4,6]. It is therefore not surprising that in mice remote territory enhancement for MB-PSGL-1 peaked early since P-selectin mobilization from Wiebel-Palade bodies occurs rapidly and peaks early after injury [14]; whereas enhancement for MB-PS was later because MP-PS retention relies largely on leukocyte attachment which peaks later [15].

In canine experiments, very high remote territory enhancement was found which made spatial definition of the risk area difficult in some cases. We believe this finding is from inflammation from prolonged open-chest exposure, a notion supported by results from closed-chest experiments. One could argue that this remote area enhancement indicates that MCE with Sonazoid has the sensitivity to detect even the small amount of injury from the surgical preparation.

With regards to mechanism for MB-PS retention, intravital microscopy demonstrated attachment to both activated adherent leukocytes and to the activated endothelium. Flow cytometry with in vitro binding in human serum confirmed that complement was a predominate mechanism for cellular

attachment. This finding is not surprising because complement-mediated recognition is thought to be the normal reticuloendothelial mechanism for lipid microbubble clearance from the blood and also for the normal late "phagocytic" phase on liver contrast ultrasound [16]. Extensive testing of liposomal drug preparations has led to a detailed understanding of the interaction of complement proteins and non-self membranes, the effect of lipid excipient charge, and in particular the effect of PS to accelerate opsonization [17-19]. We previously demonstrated that PS enhances MB leukocyte attachment and microvascular retention [11], and that anionic MB retention is reduced in animals genetically deficient for C3 [20]. In this study, we definitively demonstrated that the leukocyte-MB-PS interaction relies largely on C3 which is the predicted mediator of opsonization. The C1q component was found to be critical and, although it has been shown to also mediate opsonization [21], our data showing near complete elimination of attachment with C3-depleted serum suggest that the role C1q played was as an initiator of the complement cascade. There was only a minor role for scavenger receptors.

STUDY LIMITATIONS. With regards to the mechanism of MB retention, we demonstrated the critical role of complement for leukocyte attachment but not for

FIGURE 4   Flow Cytometry of Phosphatidylserine Attachment to Leukocytes
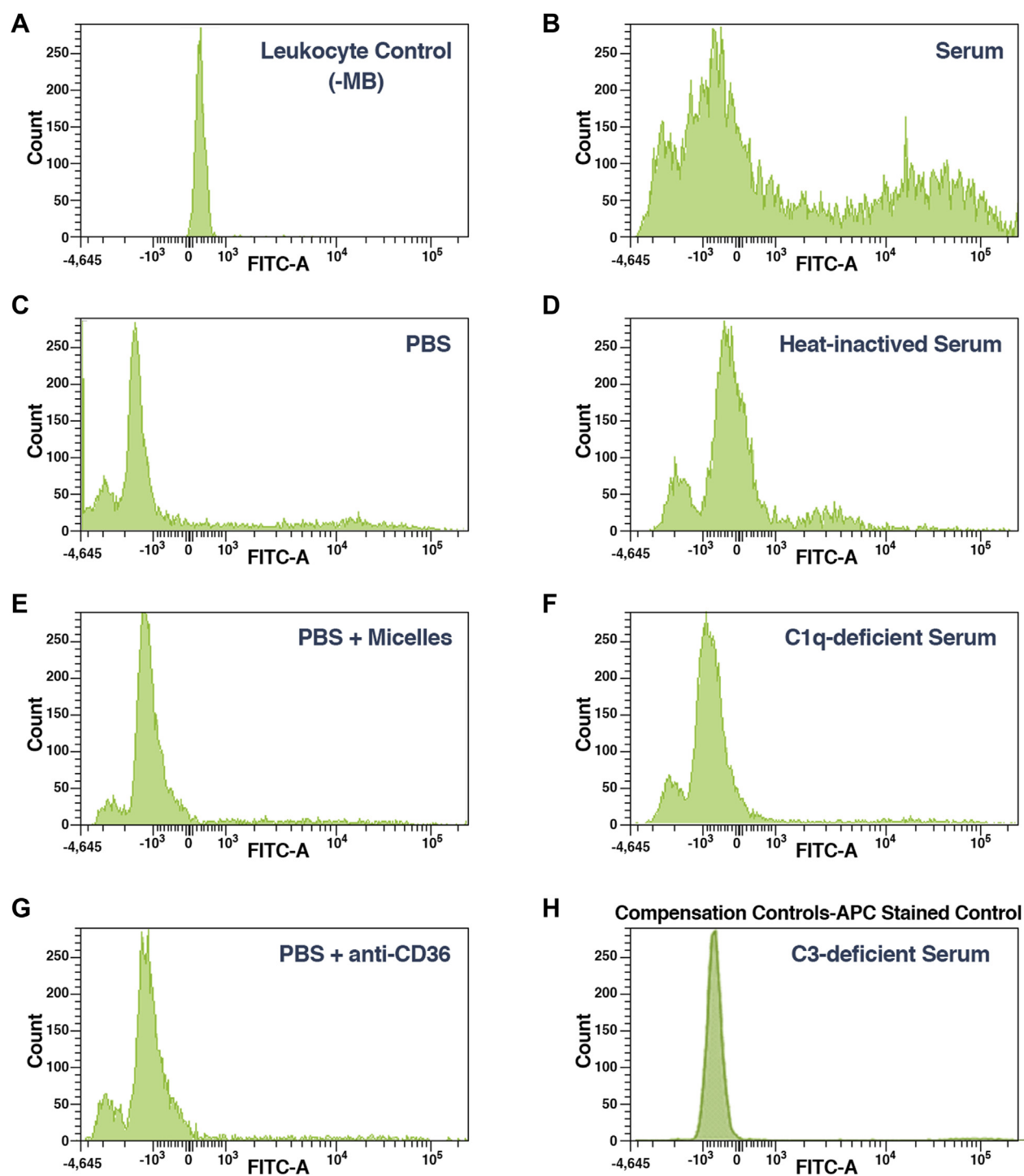
Flow cytometry gated solely to leukocytes by both side-forward scatter and allophycocyanin (APC) — labeled anti-CD45 staining (Online Figure 1). **(A)** Monocytes and neutrophils labeled with APC exhibited minimal fluorescence in the fluorescein isothiocyanate conjugated (FITC) range. **(B to H)** DiO-labeled phosphatidylserine microbubbles (MB-PS) attachment to leukocytes (FITC fluorescence >1O3) in different conditions illustrating the critical role of serum complement for leukocyte-MB-PS interaction. Online Videos 1 and 2 demonstrate in vivo attachment of MB-PS to leukocytes and the endothelium in the microcirculation of post-ischemic muscle. PBS = phosphate-buffered saline.

endothelial cells. However, previous studies have suggested that endothelial attachment of lipid microbubbles in other tissues (aorta, kidney) is mediated at least in part by complement. Because of the striking flow cytometry results with complement-depleted serum, we did not test the effects of blocking other recognized PS-receptors such as CD68 and CD91. With regards to spatial assessment of the risk area in mice, we believe the presence of sternal attenuation with high frequency imaging limited us from having a tighter relationship with microsphere data. In the canine experiments, MCE molecular imaging was performed in a model of infarction rather than simply brief ischemia and very late post-ischemic imaging was not performed because the model was governed by the opportunity to add these experiments as a supplement to a separate protocol. Although the degree of ischemia in this model was severe, we are still reassured by the finding of Sonazoid signal enhancement in the noninfarcted post-ischemic myocardium in a large mammalian model. Finally, only in human trials will we be able to evaluate whether the targeting of vascular inflammation is specific for post-ischemic changes or will also become positive, but also potentially useful, in other conditions such as active myocarditis, transplant rejection, or myocarditis.

CONCLUSIONS

We have demonstrated that MCE ischemic memory imaging even in noninfarcted tissue is possible using the complement-mediated interaction between PS-containing microbubbles. The degree of signal enhancement is robust and similar to that produced by selectin-targeted agent. These pre-clinical experiments form the basis for the potential investigation for diagnostic imaging of inflammation and injury, including myocardial ischemia, using agents that are feasible for human use.

REPRINT REQUESTS AND CORRESPONDENCE: Dr. Jonathan R. Lindner, Knight Cardiovascular Institute, UHN-62, Oregon Health & Science University, 3181 SW Sam Jackson Park Road, Portland, Oregon 97239. E-mail: lindnerj@ohsu.edu.

PERSPECTIVES

COMPETENCY IN PATIENT CARE AND PROCEDURAL SKILLS: The symptoms that prompt patients with acute coronary syndromes to seek medical attention are often nonspecific in nature. Accordingly, tests for detecting myocellular injury or necrosis (e.g., electrocardiogram and troponins) have been incorporated into clinical practice. These basic tools for risk stratification also have limitations in their diagnostic accuracy. Imaging techniques for ischemic memory imaging are being developed to address the need to detect recent but resolved ischemia without necrosis, and for evaluating spatial extent of the myocardial area involved. The results of this study indicate that echocardiographic detection of vascular activation using myocardial microvascular retention of ultrasound contrast material can be used to detect brief recent ischemia. This may provide a rapid bedside technique that improves patient care by rapid detection or exclusion of acute coronary syndrome in patients.

TRANSLATIONAL OUTLOOK: The major impact on patient care of this study is the finding that a simple chemical modification of the lipid microbubble shell (the addition of phosphatidylserine) results in an ability to detect recently ischemia equivalent to that provided by a surface conjugation of a ligand that targets microbubbles to a specific endothelial markers of activation. The importance of this finding is underscored by the availability of an agent already used in humans that contains the lipid moiety that enhances post-ischemic microvascular retention.

REFERENCES

1. Brieger D, Eagle KA, Goodman SG, et al. Acute coronary syndromes without chest pain, an underdiagnosed and undertreated high-risk group: insights from the Global Registry of Acute Coronary Events. Chest 2004;126:461–9.

2. Mehta RH, Eagle KA. Missed diagnoses of acute coronary syndromes in the emergency room–continuing challenges. N Engl J Med 2000;342:1207–10.

3. Taegtmeyer H, Dilsizian V. Imaging myocardial metabolism and ischemic memory. Nat Clin Pract Cardiovasc Med 2008;5 Suppl 2:S42–8.

4. Kaufmann BA, Lewis C, Xie A, Mirza-Mohd A, Lindner JR. Detection of recent myocardial ischaemia by molecular imaging of P-selectin with

targeted contrast echocardiography. Eur Heart J 2007;28:2011–7.

5. Villanueva FS, Lu E, Bowry S, et al. Myocardial ischemic memory imaging with molecular echocardiography. Circulation 2007;115:345–52.

6. Davidson BP, Kaufmann BA, Belcik JT, Xie A, Qi Y, Lindner JR. Detection of antecedent myocardial ischemia with multiselectin molecular imaging. J Am Coll Cardiol 2012;60:1690–7.

7. Davidson BP, Chadderdon SM, Belcik JT, Gupta S, Lindner JR. Ischemic memory imaging in nonhuman primates with echocardiographic molecular imaging of selectin expression. J Am Soc Echocardiogr 2014;27:786–93.e2.

8. Lindner JR, Coggins MP, Kaul S, Klibanov AL, Brandenburger GH, Ley K. Microbubble persistence in the microcirculation during ischemia/reperfusion and inflammation is caused by integrin- and complement-mediated adherence to activated leukocytes. Circulation 2000;101:668–75.

9. Lindner JR, Dayton PA, Coggins MP, et al. Noninvasive imaging of inflammation by ultrasound detection of phagocytosed microbubbles. Circulation 2000;102:531–8.

10. Tsutsui JM, Xie F, Cano M, et al. Detection of retained microbubbles in carotid arteries with real-time low mechanical index imaging in the setting

of endothelial dysfunction. J Am Coll Cardiol 2004;44:1036–46.

11. Lindner JR, Song J, Xu F, et al. Noninvasive ultrasound imaging of inflammation using microbubbles targeted to activated leukocytes. Circulation 2000;102:2745–50.

12. Christiansen JP, Leong-Poi H, Klibanov AL, Kaul S, Lindner JR. Noninvasive imaging of myocardial reperfusion injury using leukocyte-targeted contrast echocardiography. Circulation 2002;105:1764–7.

13. Behm CZ, Kaufmann BA, Carr C, et al. Molecular imaging of endothelial vascular cell adhesion molecule-1 expression and inflammatory cell recruitment during vasculogenesis and ischemia-mediated arteriogenesis. Circulation 2008;117:2902–11.

14. Ley K, Bullard DC, Arbones ML, et al. Sequential contribution of L- and P-selectin to leukocyte rolling in vivo. J Exp Med 1995;181:669–75.

15. Dreyer WJ, Michael LH, West MS, et al. Neutrophil accumulation in ischemic canine

myocardium. Insights into time course, distribution, and mechanism of localization during early reperfusion. Circulation 1991;84:400–11.

16. Yanagisawa K, Moriyasu F, Miyahara T, Yuki M, Iijima H. Phagocytosis of ultrasound contrast agent microbubbles by Kupffer cells. Ultrasound Med Biol 2007;33:318–25.

17. Szebeni J, Muggia F, Gabizon A, Barenholz Y. Activation of complement by therapeutic liposomes and other lipid excipient-based therapeutic products: prediction and prevention. Adv Drug Deliv Rev 2011;63:1020–30.

18. Devine DV, Wong K, Serrano K, Chonn A, Cullis PR. Liposome-complement interactions in rat serum: implications for liposome survival studies. Biochim Biophys Acta 1994;1191: 43–51.

19. Huong TM, Ishida T, Harashima H, Kiwada H. The complement system enhances the clearance of phosphatidylserine (PS)-liposomes in rat and guinea pig. Int J Pharm 2001;215:197–205.

20. Fisher NG, Christiansen JP, Klibanov A, Taylor RP, Kaul S, Lindner JR. Influence of microbubble surface charge on capillary transit and myocardial contrast enhancement. J Am Coll Cardiol 2002;40:811–9.

21. Nauta AJ, Castellano G, Xu W, et al. Opsonization with C1q and mannose-binding lectin targets apoptotic cells to dendritic cells. J Immunol 2004;173:3044–50.

22. Sontum PC. Physicochemical characteristics of Sonazoid, a new contrast agent for ultrasound imaging. Ultrasound Med Biol 2008;34:824–33.

KEY WORDS complement, microbubbles, myocardial contrast echocardiography, myocardial ischemia, phosphatidylserine

---

▓ **APPENDIX** For a supplemental figure and videos, please see the online version of this article.